

EXPLORING POSSIBLE ROLES OF ORGANIC ANION-TRANSPORTING  
POLYPEPTIDES IN INVADOPODIA FUNCTION

by

George Travis Tabor

Honors Thesis

Appalachian State University

Submitted to the A. R. Smith Department of Chemistry

and the Honors College

in partial fulfillment of the requirements for the degree of

Bachelor of Science

May, 2016

Approved by:

---

Jennifer Cecile, Ph.D., Thesis Director

---

Carol Babyak, Ph.D., Second Reader

---

Darren Seals, Ph.D., Third Reader

---

Libby Puckett, Ph.D., Departmental Honors Director

---

Ted Zerucha, Ph.D., Interim Director, The Honors College

## Table of Contents

<b>I. List of Figures and Tables.....</b>	<b>3</b>
<b>II. List of Abbreviations .....</b>	<b>4</b>
<b>III. Abstract.....</b>	<b>5</b>
<b>IV. Introduction.....</b>	<b>7</b>
<b>V. Methods .....</b>	<b>14</b>
<i>Cell culture.....</i>	<b>14</b>
<i>Fluorescence transport assay: Overview and optimization .....</i>	<b>14</b>
<i>OATP uptake inhibition assays .....</i>	<b>19</b>
<i>Androgen receptor stimulation in Src-3T3 cells.....</i>	<b>20</b>
<i>Fluorescence microscopy.....</i>	<b>20</b>
<i>Data analysis.....</i>	<b>21</b>
<b>VI. Results.....</b>	<b>22</b>
<i>OATP fluorescent substrate uptake screen.....</i>	<b>22</b>
<i>Time course of rhodamine-123 uptake by PC3 cells.....</i>	<b>23</b>
<i>OATP inhibition assays .....</i>	<b>24</b>
<b>VII. Discussion.....</b>	<b>29</b>
<b>VIII. Future Work.....</b>	<b>34</b>
<b>IX. Conclusion .....</b>	<b>36</b>
<b>X. Acknowledgements .....</b>	<b>37</b>
<b>XI. Biographical Sketch .....</b>	<b>38</b>
<b>XII. References .....</b>	<b>39</b>

## I. List of Figures and Tables

Figure 1. Invadopodia structure and function in murine fibroblasts overexpressing constitutively active Src.	8
Figure 2. Fold recognition model of OATP1B1 and OAT1.	9
Figure 3. Proposed mechanism for OATP-AR-Src signaling in invadopodia formation and function.	12
Figure 4. Chemical structure of rhodamine-123 (Rh-123).	13
Figure 5. Overview of the initial fluorescence transport assay protocol for mammalian cell lines.	16
Figure 6. Fluorescence transport assay lysis buffer analysis.	17
Figure 7. Optimized fluorescence transport assay protocol overview.	18
Figure 8. Uptake of OATP substrate dyes by Src-3T3, PC3, and MDA-MB-231 cell lines.	22
Figure 9. Uptake of selected OATP substrate dyes by Src-3T3, PC3, and MDA-MB-231 cell lines.	23
Figure 10. Time course of rhodamine-123 uptake by PC3 cells.	24
Figure 11. Effect of temperature on uptake of rhodamine-123 by MDA-MB-231 cells.	25
Figure 12. Effects of OATP inhibitors on long-term rhodamine-123 uptake by PC3 cells.	26
Figure 13. Effects of OATP inhibitors on early rhodamine-123 uptake by PC3 cells.	27
Figure 14. Effects of OATP inhibitors on early rhodamine-123 uptake by LNCaP cells grown in androgen-depleted conditions.	28
Figure 15. Overview of the gelatin degradation assay protocol.	34
Table I. Spectroscopic and kinetic data for OATP fluorescent substrates.	15
Table II. List of OATP inhibitors and their relevant targets.	19

## II. List of Abbreviations

- Acetoxymethyl ester derivative of Fluo-3 (Fluo-3 AM)
- Androgen-deprivation therapy (ADH)
- Androgen receptor (AR)
- Caveolin-1 (Cav-1)
- Dehydroepiandrosterone sulfate (DHEAS)
- 4',6-diamidino-2-phenylindole (DAPI)
- Dulbecco's Modified Eagle Medium (DMEM)
- Estrone-3-sulfate (E3S)
- Extracellular matrix (ECM)
- Fluorescein-methotrexate (FMTX)
- Hank's Balanced Salt Solution (HBSS)
- Human Embryonic Kidney Cells (HEK293)
- Lipid raft domain (LRD)
- LNCaP cells overexpressing Tks5 (LNPT)
- Membrane type-1 matrix metalloproteinase (MT1-MMP)
- Murine embryonic fibroblast cell line (NIH-3T3)
- NIH-3T3 cells stably overexpressing constitutively active Src (Src-3T3)
- Organic anion transporter (OAT)
- Organic anion-transporting polypeptide (OATP)
- P-glycoprotein (p-gp)
- Rhodamine-123 (Rh-123)
- Roswell Park Memorial Institute Media (RPMI)

### **III. Abstract**

Drug resistant, invasive tumors are among the most devastating cancers. It is the goal of this project to explore the potential relationships between these two phenotypes in a variety of tissue culture model systems. Invadopodia are actin-rich protrusions of the cellular membrane involved in extracellular matrix remodeling that allow cancer cells to invade other tissues during metastasis. Organic anion transporting-polypeptides (OATPs) mediate xenobiotic exchange across the cellular membrane and are believed to colocalize with lipid raft domains (LRDs) and caveolin-1 in humans, two factors that are also required for invadopodia function in breast cancer and melanoma cells. These transporters are thought to contribute to the multi-drug resistance phenotype of stubborn tumors and are upregulated in multiple cancer cell lines.

To determine if functional OATPs are present in invadopodia-competent cells, fluorescence transport assays were performed on human prostate (PC3, LNCaP) and breast (MDA-MB-231) cancer cells as well as a murine fibroblast (NIH-3T3) cell line overexpressing constitutively active Src (Src-3T3). All cell lines exhibited robust uptake of rhodamine-123 (Rh-123), a fluorescent substrate of OATP1A2. Furthermore, the uptake of Rh-123 by MDA-MB-231 and PC3 cells was likely protein-mediated as the fluorescence signals were reduced by 67% and 68% respectively when the transport assays were performed on ice. In addition, an inhibition assay indicated that OATP1A2 might be responsible for the observed uptake of Rh-123 by LNCaP cells grown in androgen-depleted conditions. These inhibition studies are ongoing, and future experiments will explore the ultimate

downstream effects of OATP substrates on invadopodia morphology and function. If OATPs play a role in invadopodia activity, they may contribute to the enhanced invasive phenotype of certain cancers and therefore serve as viable therapeutic targets.

#### **IV. Introduction**

From the earliest stages of conception to the final moments of life, cellular motility plays an important role in the survival of many organisms. In addition, the ability of a cell to regulate its internal composition by importing nutrients and exporting wastes allows it to flourish and adapt to changing environmental conditions. Malignant tumor cells have to ability to manipulate these “normal” cellular mechanisms in order to metastasize and resist drug treatments respectively, which frequently results in poor patient outcomes.

Invadopodia are structural features of highly aggressive cancer cells that are believed to play important roles in tumor metastasis.<sup>1</sup> These actin-dense, lipid-rich ventral protrusions of the cell membrane are known to exert motive forces on and mediate the remodeling of the extracellular matrix (ECM) (Figure 1). These processes allow a cancer cell to leave its native environment and invade other tissues during metastasis, a phenomenon that accounts for approximately 90% of cancer related deaths.<sup>2</sup>

Among the many proteins that regulate invadopodia activity, membrane type-1 matrix metalloproteinase (MT1-MMP) is especially critical for ECM degradation and remodeling.<sup>3</sup> MT1-MMP activity is regulated by caveolin-1 (Cav-1), an integral membrane protein that plays roles in endocytosis, signal transduction, vesicle transport, and migration.<sup>4</sup> Both MT1-MMP and Cav-1 are concentrated at and trafficked through cholesterol-rich regions of the cellular membrane known as lipid rafts.<sup>5</sup> Lipid rafts are membrane domains comprised of sphingolipids and proteins that exhibit some degree of segregation from the fluid phospholipid bilayer and are

believed to play important roles in signal transduction.<sup>6,7</sup> Invadopodia are known to be enriched in lipid rafts and caveolin-1, which are critical for the formation and function of these structures in breast cancer and melanoma cells.<sup>5,8,9</sup>

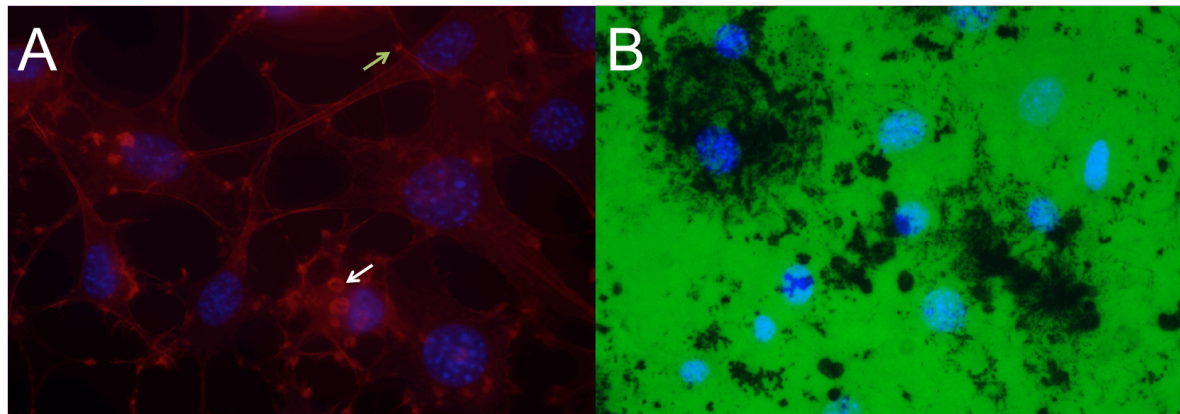


**Figure 1. Invadopodia structure and function in murine fibroblasts overexpressing constitutively active Src.** (A) Invadopodia are punctate cellular protrusions (green arrow) that form rosette superstructures (white arrow) in mature, aggressive cancer cells. Actin was stained with phalloidin 594 (red) and nuclei with DAPI (blue). (B) Gelatin degradation assays are used to score invadopodia activity. Black areas correspond to invadopodia-mediated matrix degradation. Coverslips were coated with Alexa Fluor 488-conjugated gelatin (green) to simulate extracellular matrix (ECM), and nuclei were stained with DAPI (blue).

Organic anion transporting polypeptides (OATPs) are 12-transmembrane glycoproteins that mediate the transfer of large hydrophobic organic anions across the cellular membrane (Figure 2).<sup>10</sup> Conjugated sex steroids, bile acids, drugs, and toxins are among the many substances transported by these promiscuous proteins. OATPs and organic anion transporters (OATs), a homologous class of proteins, are thought to contribute to the multi-drug resistance phenotype of stubborn cancers.<sup>11</sup>

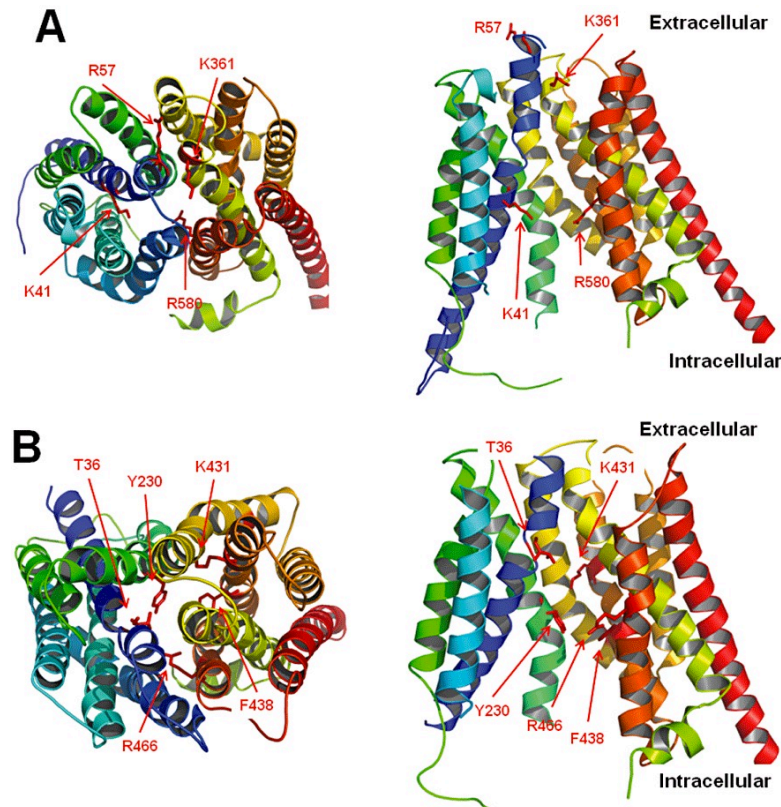


**Figure 2. Fold recognition model of OATP1B1 and OAT1.**<sup>10</sup> OATPs and OATs are homologous proteins that contain 12 transmembrane helical domains. (A) OATP1B1 and (B) OAT1 models were generated using Phyre, a protein homology recognition server.

Interestingly, OATs were found to colocalize with lipid raft domains and associate with caveolin-1 in human embryonic kidney cells.<sup>12</sup> Because OATs (and thus OATPs) are believed to exist in cellular environments consistent with those of invadopodia, we hypothesized that these transporters may be localized to and thus play a role in the formation and/or function of invadopodia. While the assumption that OATs and OATPs colocalize to similar regions of the cell may be true for some transporters, it should be noted that there is evidence that at least one OATP isoform (1B1) may not require lipid rafts for proper functioning.<sup>13</sup> This indicates that OATP expression at invadopodia may be isoform-specific.

Arawaka and coworkers observed that the OATP isoform 1A2 was upregulated in androgen receptor-positive (AR-positive) LNCaP prostate cancer cells grown in androgen-depleted conditions, which indicated a potential connection between the functions of OATPs and invadopodia.<sup>14</sup> LNCaP cells subjected to androgen-depleted conditions are studied as a model of prostate cancer in the process of becoming androgen-resistant. This period of transition is of great significance to researchers because androgen-insensitive prostate cancer is essentially untreatable since it no longer responds to androgen deprivation therapy (ADT, *i.e.* castration) and is generally more aggressive than its androgen-dependent forms.<sup>14,15</sup> OATP1A2 is known to transport dehydroepiandrosterone sulfate (DHEAS), an inactive androgen precursor produced by the adrenal glands, into prostate cells. DHEAS is eventually converted to androstenedione, a compound that activates the androgen receptor (AR), which in turn promotes cell growth and motility via genomic and extranuclear mechanisms.<sup>14,16</sup>

Since serum DHEAS concentration remains high after castration, Arakawa et al. suggested the upregulation of OATP1A2 may provide prostate cancer cells with a means to acquire alternative androgen precursors from the serum.<sup>14</sup> Thus OATP1A2-mediated transport of these precursors may contribute to the stimulation of the androgen receptor, which could promote the survival of the cancer during this period of transition.

The effects of androgen receptor stimulation on invadopodia morphology and activity have not yet been explored, but previous reports have indicated a number of interesting potential relationships (see Figure 3). For example, AR stimulation in

NIH-3T3 cells by a synthetic agonist, R1881 (methyltrienolone), increased cellular motility and induced the rapid formation of cytoskeletal ruffles and protrusions.<sup>16</sup> Other studies have implicated the activities of AR in pathways known to promote the formation of invadopodia. Src tyrosine kinase, the first discovered oncogene, is known to associate with and phosphorylate the androgen receptor in castration-resistant cancers and its upregulation has been shown to promote the formation of invadopodia in NIH-3T3 cells.<sup>17,18</sup> Furthermore, recent evidence has indicated that Src is not only upregulated in the LNCaP-derived castration-resistant prostate cancer cell line C4-2, but may actually serve to activate the AR in the absence of gonadal androgens.<sup>19</sup>

Additionally, AR stimulation has been shown to activate but not upregulate Src in PC3 cells overexpressing AR while inducing the formation of filopodial structures and promoting Boyden chamber migration (a measure of cell invasion).<sup>20</sup> Similar effects on LNCaP and C4-2 migration in response to AR stimulation were observed. While the R1881-induced increases in cellular motility and cytoskeletal rearrangements reported by Castoria et al. were believed to occur via a Src-independent pathway, it is possible that AR-activated Src may additively contribute to the formation and/or activity of invadopodia in aggressive cancer cells.<sup>16</sup> Given the crosstalk between Src, a known invadopodia promoter, and AR, a protein putatively activated by OATP1A2 substrates, future experiments will explore the role of androgens in invadopodia development. A proposed mechanism for OATP-AR-Src mediated invadopodia enhancement that combines the results of the aforementioned studies is described in Figure 3.

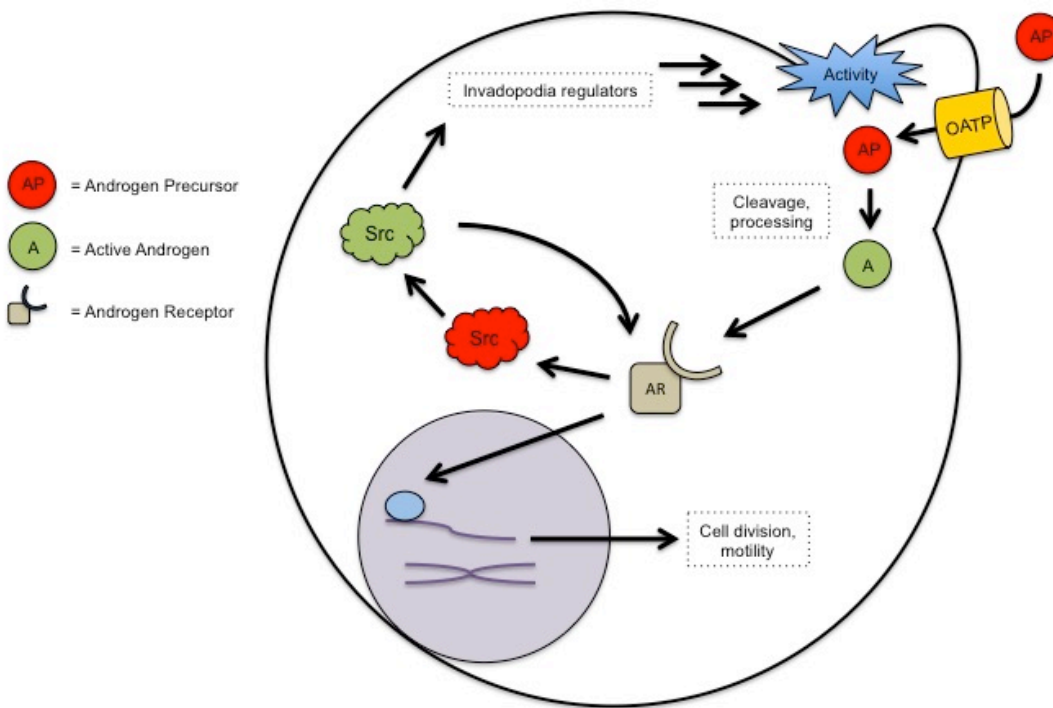


**Figure 3. Proposed mechanism for OATP-AR-Src signaling in invadopodia formation and function.** First, androgen precursor molecules like DHEAS are transported into the cell via OATP1A2 in the absence of gonadal androgens. Next, activation of the precursor molecules occurs intracellularly via cleavage and processing reactions. Stimulation of AR by these processed androgens activates Src, which in turn activates a variety of molecules required for invadopodia development and activity. OATP1A2 is localized to lipid rafts (not shown), which are concentrated in the single invadopod depicted (bulge).

These previous reports suggest that OATPs (and thus OATPs) may be localized to invadopodia and transport substances known to promote cellular motility and cytoskeletal remodeling via AR activation. It is the purpose of this project to identify and elucidate potential interactions between OATPs, their substrates, and invadopodia in a variety of cell culture models. Fluorescence transport assays were employed using OATP substrates and inhibitors to determine the presence and

identities of OATPs in multiple cancer cell lines. Human prostate (PC3, LNCaP) and breast (MDA-MD-231) cancer cells as well as a murine fibroblast cell line (NIH-3T3) stably overexpressing constitutively active Src (Src-3T3) were all observed to take up rhodamine-123 (Rh-123, Figure 4), a known substrate of OATP1A2. None of these cells took up appreciable amounts fluorescein-methotrexate (FMTX) and fluo-3, substrates of other OATP isoforms (*i.e.* 1B1 and 1B3). In addition, the uptake of Rh-123 by MDA-MB-231, PC3, and LNCaP cells was shown to be protein-mediated via a series of drug and temperature inhibition assays. Finally, a primitive inhibition assay indicated that the uptake of Rh-123 by LNCaP cells grown in androgen-depleted conditions was mediated by OATP1A2, which was consistent with a previous report.<sup>14</sup> Future experiments will explore the localization of OATPs and determine the effects of their transported substrates on invadopodia morphology and function. If OATPs are found to play a role in the development and/or activity of invadopodia, they may serve as viable therapeutic targets.

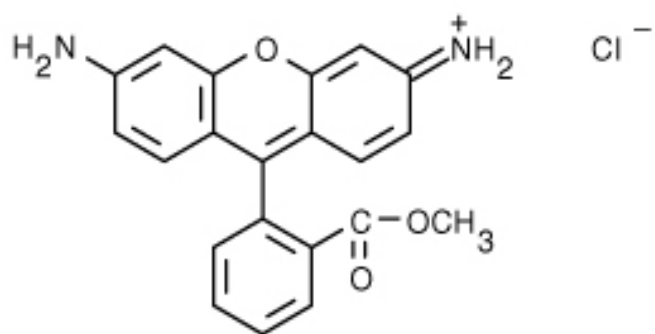


**Figure 4. Chemical structure of rhodamine-123 (Rh-123).** Rh-123 was selected as the tracer dye for assessing OATP1A2 activity in the current study. The presence of the ester group is critical for the robust fluorescence of Rh-123, which is remarkably resistant to photobleaching.<sup>21</sup> The image was retrieved from the ThermoFisher Scientific website.

## V. Methods

### *Cell culture*

The PC3 and LNCaP human prostate carcinoma cell lines were cultured in RPMI media (Sigma Aldrich, R8758) containing 10% fetal bovine serum (Sigma Aldrich, F0926) supplemented with 100 units/mL penicillin, 100 µg/mL streptomycin (Corning, 30-002-CI), 2 mM L-glutamine, 10 mM HEPES (VWR, VW1481-04), and 1 mM sodium pyruvate (Thermo Scientific, SH30239.01). Human breast carcinoma MDA-MB-231 cells were cultured in RPMI media containing 10% fetal bovine serum supplemented with 100 units/mL penicillin and 100 µg/mL streptomycin. Src-transformed NIH-3T3 cells (murine fibroblasts) were cultured in DMEM (Sigma Aldrich, D6429) containing 10% fetal bovine serum supplemented with 100 units/mL penicillin and 100 µg/mL streptomycin. All cell lines were cultured at 37°C and 5% CO<sub>2</sub>.

### *Fluorescence transport assay: Overview and optimization*

The OATP fluorescent substrate dyes, rhodamine-123 (Rh-123, ICN Biomedicals, IC15653025), fluorescein-methotrexate (FMTX, Biotium, 89138-112), and fluo-3 pentapotassium salt (Fluo-3, Biotium, 89139-176), were acquired and resuspended in DMSO (1 mM stock concentration). An old 1 mM stock of Fluo-3 AM (DMSO, Molecular Probes, F1242), a permeant derivative of Fluo-3, was used as the positive control. Log phase cells grown in 10-cm dishes were washed with 6 mL of phosphate buffered saline (Sigma Aldrich, D8537), lifted with 2 mL of 0.25% trypsin-EDTA (Sigma Aldrich, T4049), diluted with 2 mL of media, and counted using a hemocytometer. The suspensions were then diluted with an appropriate volume of

media, and  $4.0\text{--}5.0 \times 10^5$  cells were seeded into 6-well plates coated with or without poly-D-lysine (Sigma-Aldrich, P6407). These cells were incubated for 18 hours at 37°C. Next, the cells were washed three times with 1.25 mL of pre-warmed HBSS buffer (Sigma-Aldrich, H1387) on a 37°C hot plate. Two milliliters of each OATP substrate dye solution (in HBSS) were applied to the wells in triplicate. The final substrate dye concentrations (i.e.  $K_m$  values) are provided in Table I along with relevant spectroscopic and kinetic data.

**Table I. Spectroscopic and kinetic data for OATP fluorescent substrates.** The substrate solutions were prepared using the provided  $K_m$  concentrations. In the case of a dye with multiple OATP targets, the average  $K_m$  concentration was used.

<b>Substrate Dye</b>	<b>Maximum Wavelength (nm)</b>		<b>Target(s)<sup>10</sup></b>	<b><math>K_m</math> (<math>\mu\text{M}</math>)<sup>22,23</sup></b>
	<b>Excitation</b>	<b>Emission</b>		
Rh-123	506	529	OATP1A2	0.3
FMTX	496	516	OATP1B1	5.2
			OATP1B3	8.9
Fluo-3	506	526	OATP1B3	2.3
Fluo-3 AM (+)	488	525	Permissible	N/A

After incubating for 30 minutes at 37°C, the cells were washed three times with 1.25 mL of 4°C HBSS buffer. To each well, 300  $\mu\text{L}$  of 1M NaOH were added, and the cells were manually lysed using a Corning scraper. The plates were again covered and incubated at 37°C for 1 hour. The lysates were then neutralized with 50  $\mu\text{L}$  of 6 M HCl. Bradford assays were performed using 10  $\mu\text{L}$  of each sample to determine the respective protein concentrations (Bio-Rad). A calibration curve was constructed from triplicate measurements of 1, 2, 3, 4, and 5  $\mu\text{g}$  bovine serum albumin (BSA) standards and absorbance at 595 nm was measured using a VersaMax plate reader (Molecular Devices, BNR05610). One hundred microliters of

each sample were transferred to a black 96-well plate in duplicate or triplicate. These samples were excited with 485 nm light and the emission at 535 nm was measured using a Tecan Infinite F500 microplate reader. The fluorescence intensities were then normalized to protein concentrations. An overview of the initial fluorescence transport assay protocol is outlined in Figure 5.

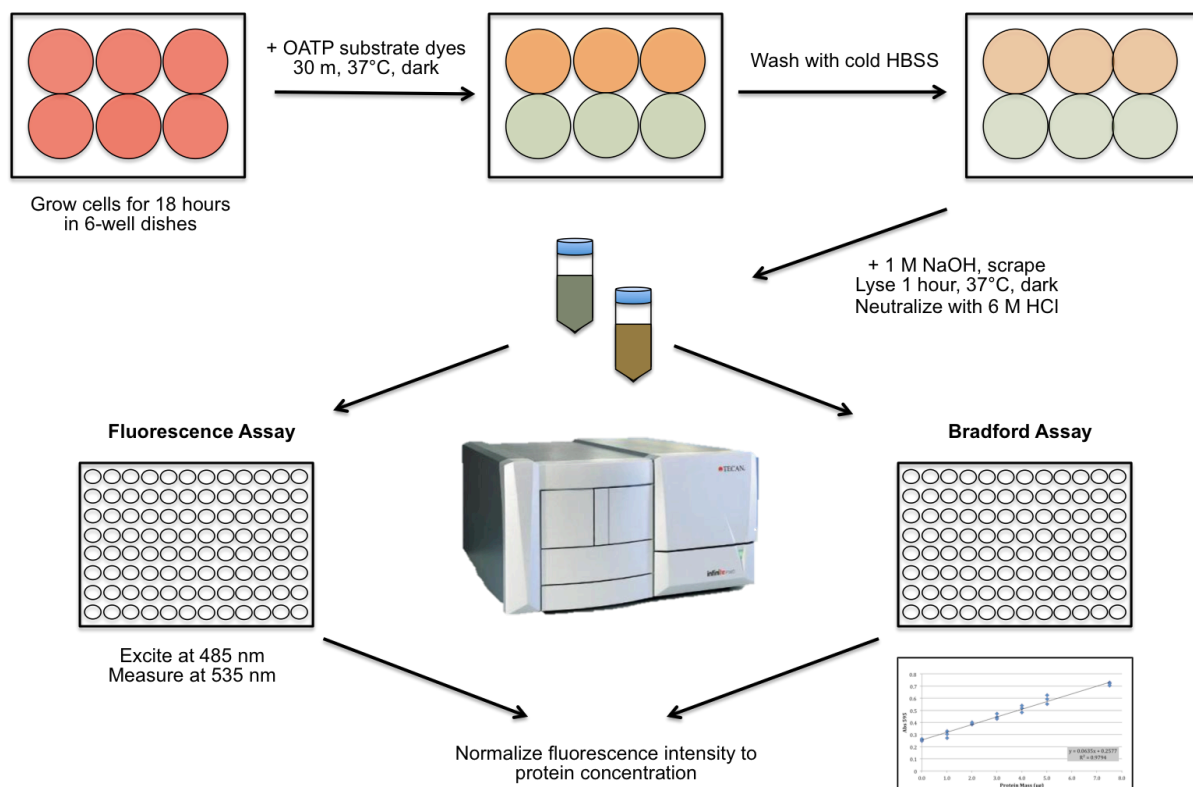


**Figure 5. Overview of the initial fluorescence transport assay protocol for mammalian cell lines.**

After performing replicate experiments of the aforementioned fluorescence transport assay protocol, it became apparent that there was an issue with the reproducibility of the results (compare the magnitudes of the normalized Rh-123 fluorescence signals of MDA-MB-231 in Figures 8 and 11). While the overall trends between trials were similar, the magnitudes of the fold normalized fluorescence values varied widely.

Due to the drastic reduction in Rh-123 fluorescence intensity above and below pH values of 12 and 1, respectively, it was surmised that the strong base lysis system may not be appropriate for use with this dye.<sup>21,24</sup> In order to reduce the possible pH effects on Rh-123 fluorescence, a detergent-based lysis buffer was employed. Efficient lysis was achieved with 1% Triton X-100/HBSS and the effect of the detergent on Rh-123 fluorescence was determined by creating a dilution curve of the dye in both empty and detergent-containing buffers. The presence of 1% Triton X-100 reduced Rh-123 fluorescence significantly only at dye concentrations greater than 0.5  $\mu$ M (Figure 6).

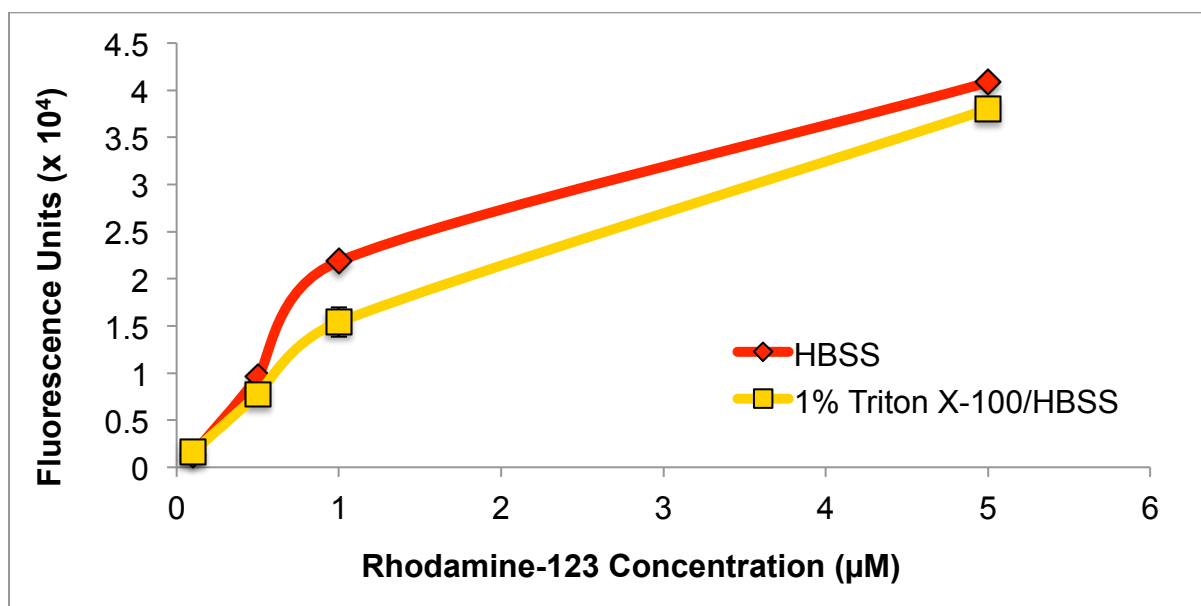


**Figure 6. Fluorescence transport assay lysis buffer analysis.** The presence of 1% Triton X-100 detergent reduced Rh-123 fluorescence compared to that in empty buffer at high dye concentrations. Data are average fluorescence unit values with standard deviations from triplicate measurements at each concentration.

After the lysis buffer was optimized, the protein assay step was omitted. Instead of normalizing fluorescence to protein concentration, the fluorescence values were inherently normalized to the number of cells plated at the onset of the

experiment. This reduced the experimental time and thus improved the efficiency of the assay significantly. Furthermore, after completing the time course of Rh-123 uptake assay (See Figure 10), the incubation step was reduced to 5 minutes. The optimized fluorescence transport assay protocol is illustrated in Figure 7.

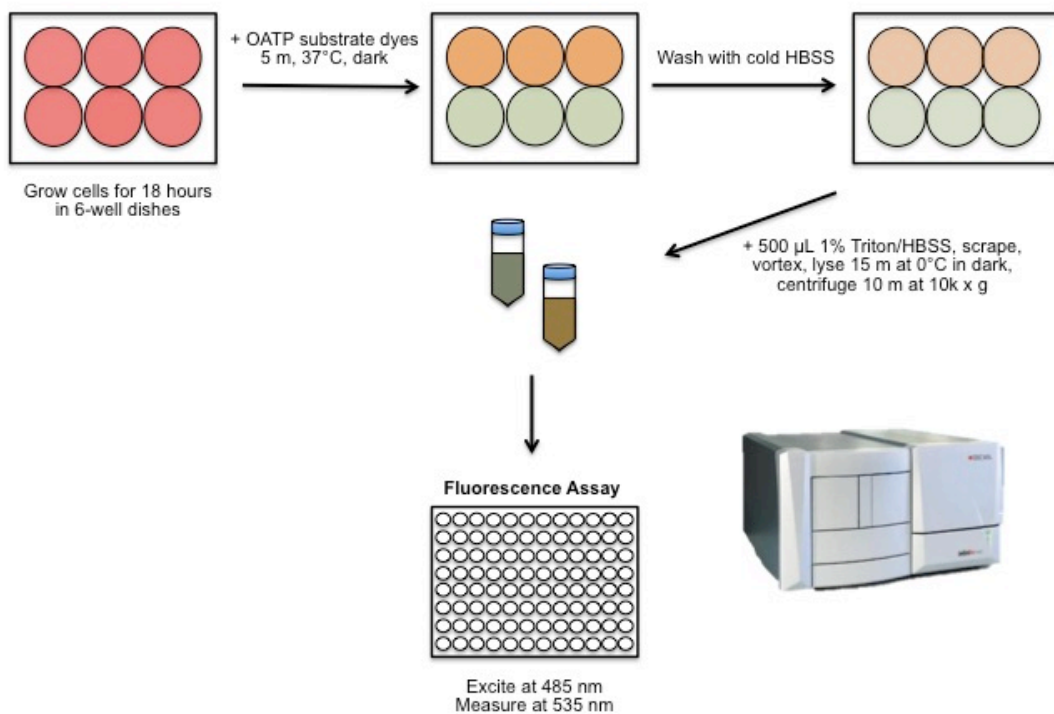


**Figure 7. Optimized fluorescence transport assay protocol overview.**

### *OATP uptake inhibition assays*

Stock solutions of sodium taurocholate (10 mM, dH<sub>2</sub>O, Alfa, A18346), rifampin (10 mM, DMSO, Alfa, J60836), estrone-3-sulfate (12.6 mM, methanol, Sigma, 438-67-5), and ketoconazole (20 mM, DMSO, MP Pharmaceuticals, 159158) were prepared in the indicated solvent. For the PC3 inhibition assays, cells were simultaneously exposed to the inhibitor and Rh-123 during the incubation step. During the androgen-depleted LNCaP inhibition assay, the cells were incubated with the indicated inhibitors for 10 minutes before being exposed to the dye. In addition, for the LNCaP assay, the 6-well plates were coated with 50 mg/mL poly-L-lysine for one hour and then washed twice with PBS prior to seeding in order to improve cell adhesion. The final concentrations of the inhibitors and their OATP targets are provided in Table II.

**Table II. List of OATP inhibitors and their relevant targets.**

Inhibitor	Targets <sup>10,25</sup>	Stock Solvent	Final Concentration (mM)
Sodium taurocholate	OATP1A2, OATP1B1, OATP1B3, OAT3	dH <sub>2</sub> O	0.3
Rifampin	OATP1A2, OATP1B1, OATP1B3	DMSO	0.1
Estrone-3-Sulfate	OATP1A2, OATP1B1, OATP1B3, OAPT1C1	Methanol	0.3
Ketoconazole	OATP1A2, OATP1B1, OAT1	DMSO	0.3

### *Androgen receptor stimulation in Src-3T3 cells*

NIH-3T3 fibroblasts stably expressing constitutively active Src (Src-3T3) were grown in either normal media or media containing charcoal-stripped serum for three days. Into 12-well dishes,  $1.4 \times 10^5$  cells of each condition were seeded and incubated for 12 hours at 37°C in the appropriate media. When the cells were approximately 60-80% confluent, they were challenged with 10 and 100 nM solutions of R1881 synthetic androgen receptor agonist (with a final ethanol concentration of 0.0001% (v/v) in the appropriate media). The treatments were incubated at 37°C for 20 minutes, 1 hour, and 6 hours.

### *Fluorescence microscopy*

Coverslips were washed twice with 1X PBS, fixed with 0.3% formaldehyde/PBS for 10 minutes, washed twice more with PBS, and stored at 4°C until all slips were processed at once. Next, the slips were permeabilized with 0.1% Triton X-100/PBS for 10 minutes with gentle rocking and washed with PBS for five minutes three times. The slips were then washed in 0.1% Tween/PBS for 5 minutes and inverted on 50 µL drops of an actin stain mixture consisting of 1:200 (v/v) Alexa Fluor 488 phalloidin (Molecular Probes, A-12379) and 5% donkey serum in PBS. After one hour of incubation at room temperature in the dark, the slips were washed three times in PBS and mounted on glass slides using ProLong Gold Plus DAPI (Life Technologies, P36935). The slips were left to dry overnight and invadopodia morphology was imaged using an Olympus BX51 fluorescent microscope in conjunction with QCapture software (version 2.9.13). Images were processed and analyzed using ImageJ software (version 1.48).<sup>26</sup>

### *Data analysis*

Unless otherwise indicated, all uncertainty values were determined using the method of partial derivatives with Maple 2015. The standard deviation of technical replicates was used as the uncertainty value of each biological replicate.

## VI. Results

### OATP fluorescent substrate uptake screen

In an initial attempt to determine if invadopodia-competent cancer cell lines expressed functional OATPs, a series of fluorescence transport assays were performed on a variety of cell lines using known fluorescent substrate dyes. The uptake of three OATP substrate dyes, rhodamine-123 (Rh-123), fluorescein-methotrexate (FMTX), and fluo-3 by Src-3T3, PC3, and MDA-MB-231 cell lines was assessed using the initial fluorescence transport assay protocol. Robust uptake of rhodamine-123 was observed in all three cell lines (Figure 8).

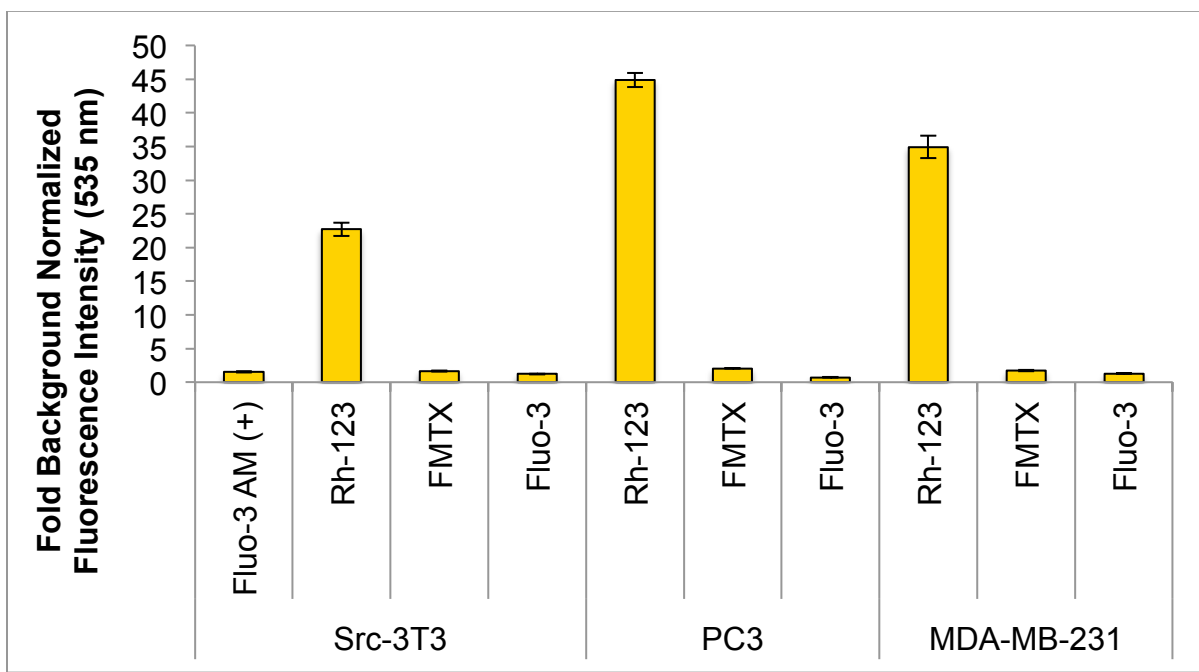


**Figure 8. Uptake of OATP substrate dyes by Src-3T3, PC3, and MDA-MB-231 cell lines.** Data are the fold background normalized fluorescence intensities at 535 nm from a single, representative experiment ( $n = 1$ ). Each cell line tested took up rhodamine-123 (Rh-123), a fluorescent substrate of OATP1A2. Transport of FMTX and fluo-3 was significantly lower than that of Rh-123.

While Rh-123 was shown to accumulate in all cell lines tested, it was unclear whether the fluorescence signal of the FMTX and fluo-3 treatments were significantly

different from the background (Figure 9). While the acetoxyethyl ester derivative of fluo-3 (fluo-3 AM) is a permissible dye that would be expected to easily pass through the cell membrane, the stock used in this experiment was old. This could explain the low fluorescence intensity of the corresponding cell lysate. In addition, the fluorescence transport assay protocol used in this study was not exactly like the one published by ThermoFisher Scientific for AM dyes, which could have resulted in suboptimal fluorescence intensities.<sup>27</sup>

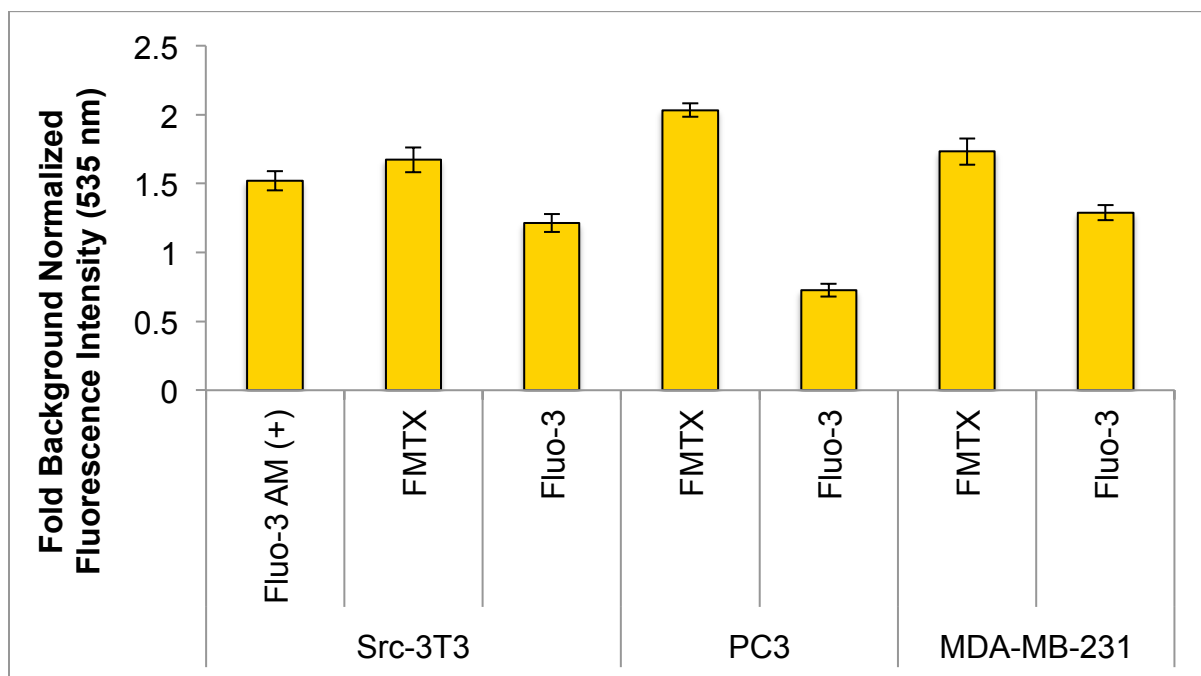


**Figure 9. Uptake of selected OATP substrate dyes by Src-3T3, PC3, and MDA-MB-231 cell lines.** Data are identical to that in Figure 8 with the Rh-123 treatments removed. Further replicates would be required to determine if the signal from the FMTX and fluo-3 samples are significantly different from that of the background ( $n = 1$ ).

#### *Time course of rhodamine-123 uptake by PC3 cells*

In order to achieve a rough understanding of the kinetics of Rh-123 uptake by PC3 cells, a time course experiment was performed using the optimized

fluorescence transport assay protocol with incubation times of 2.5, 5, and 10 minutes. PC3 cells were observed to accumulate Rh-123 most rapidly within the first two minutes of incubation, after which the uptake increased at a decreasing rate (Figure 10). This trend would be expected for protein-mediated transport as passive uptake would be considerably slower.<sup>23</sup>

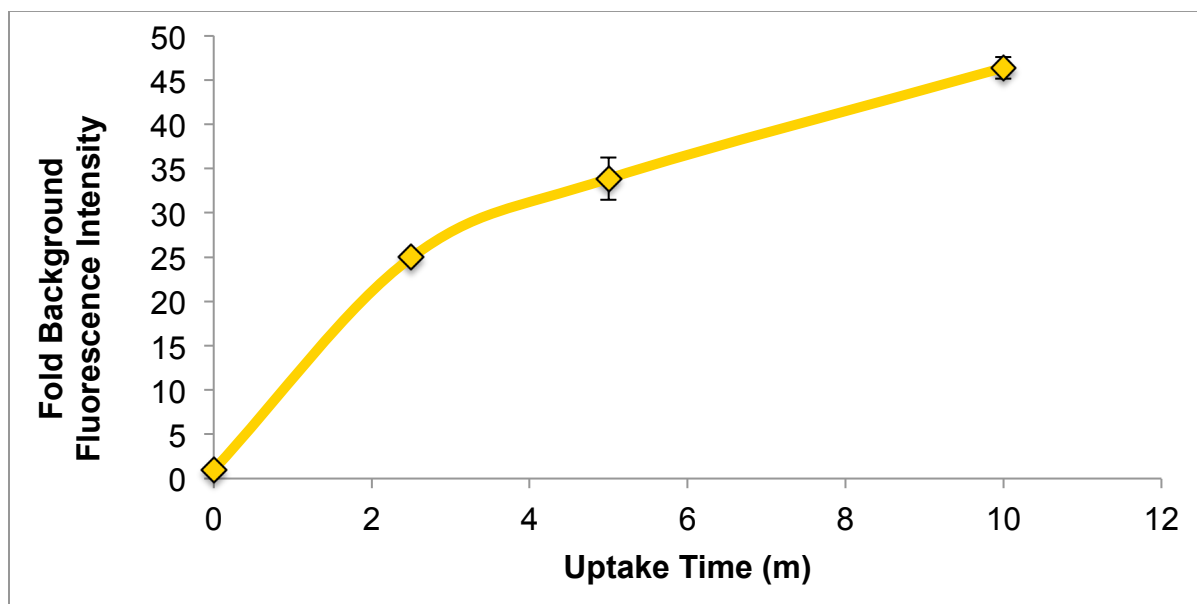


**Figure 10. Time course of rhodamine-123 uptake by PC3 cells.** PC3 cells were demonstrated to take up Rh-123 rapidly within the first 5 minutes of incubation. The decreasing slope of the curve indicated intracellular Rh-123 may reach its equilibrium concentration after 30 minutes. Standard deviations from 3 replicates of each time point are shown.

#### OATP inhibition assays

In order to further determine if the uptake of Rh-123 by MDA-MB-231 cells was protein-mediated or a product of simple diffusion, fluorescence transport assays were performed at physiological temperature and on ice using the initial protocol with a 30 minute incubation period. Since cellular proteins only function properly within a narrow temperature range, it was assumed that the cold treatment would reduce

transporter activity more than it would affect passive diffusion through the phospholipid bilayer. As shown in Figure 11, the cold treatment fluorescence signal of the MDA-MB-231 lysate was 67% intense than that of the 37°C treatment.

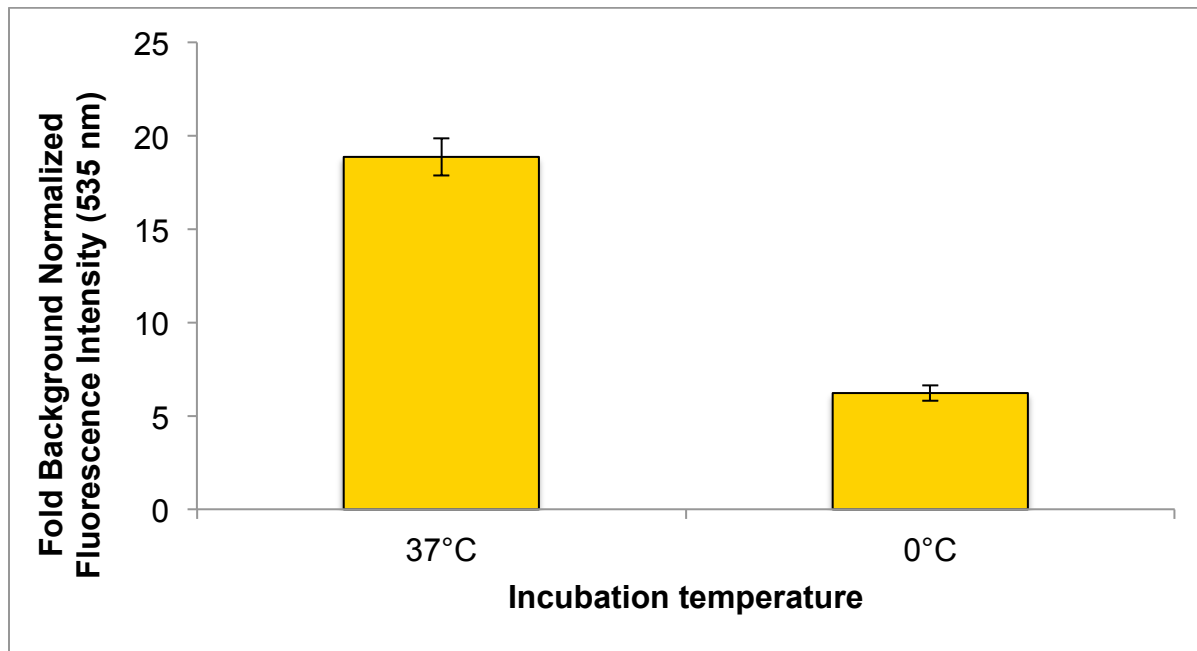


**Figure 11. Effect of temperature on uptake of rhodamine-123 by MDA-MB-231 cells.** Uptake of rhodamine-123 by MDA-MB-231 cells was significantly reduced under cold conditions ( $n = 1$ ). The fluorescence intensity at 535 nm of the cold treatment lysate was 67% less than that of the 37°C treatment lysate.

The results of the time course experiment and initial ice inhibition assay indicated that the uptake of Rh-123 by PC3 and MDA-MB-231 cells was protein-mediated. In order to identify the transporter(s) responsible for this uptake, a series of fluorescence transport assays (optimized protocol) were performed in which a variety of known OATP inhibitors were introduced in presumably saturating quantities during the incubation step. As shown in Figure 12, neither rifampin (0.1 mM) nor sodium taurocholate (0.3 mM) were shown to inhibit Rh-123 uptake by PC3 cells at the concentrations used in this experiment. Furthermore, it appeared that sodium taurocholate might have actually inhibited dye export as it increased the

intracellular Rh-123 concentration. Also shown are the results from an ice inhibition assay performed in tandem with the drug inhibitor treatments. The fluorescence signal of the ice treatment lysate was 68% lower than that of the 37°C treatment.

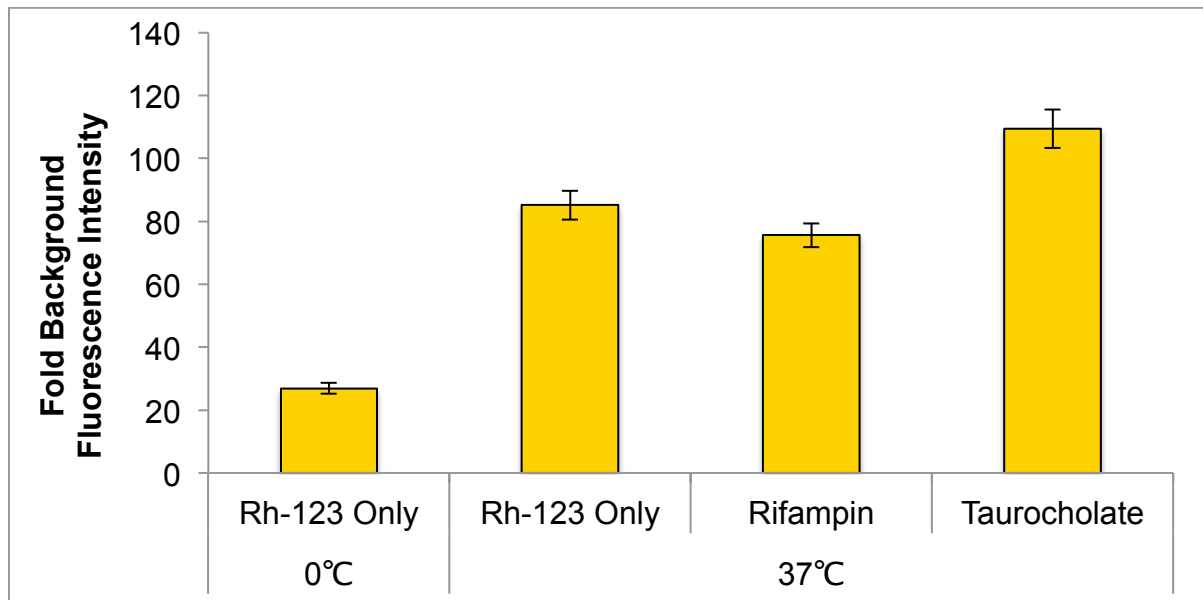


**Figure 12. Effects of OATP inhibitors on long-term rhodamine-123 uptake by PC3 cells.** Rh-123 uptake by PC3 cells was not significantly inhibited by rifampin (0.1 mM) or sodium taurocholate (0.3 mM) during the 30 minute incubation step at 37°C. Also shown is the inhibition of Rh-123 uptake by PC3 cells in cold conditions. Here the fluorescence signal of the ice treatment lysate was 68% lower than that of the 37°C condition. Data are the mean fold background fluorescence intensities and standard deviations of three biological replicates for each treatment. Each biological replicate value was the mean of three technical replicates ( $n = 1$ ).

After considering the results of the time-course assay that indicated an import/export equilibrium may have been established after a 30 minute incubation step, a series of OATP inhibition assays were performed using an incubation step of five minutes (optimized protocol). As shown in Figure 13, rifampin (0.1 mM) and taurocholate (0.3 mM) did not inhibit apparent Rh-123 uptake by PC3 cells at this time point. Furthermore, the presence of estrone-3-sulfate (E3S) appeared to increase the amount of intracellular Rh-123, presumably by inhibiting an exporter.

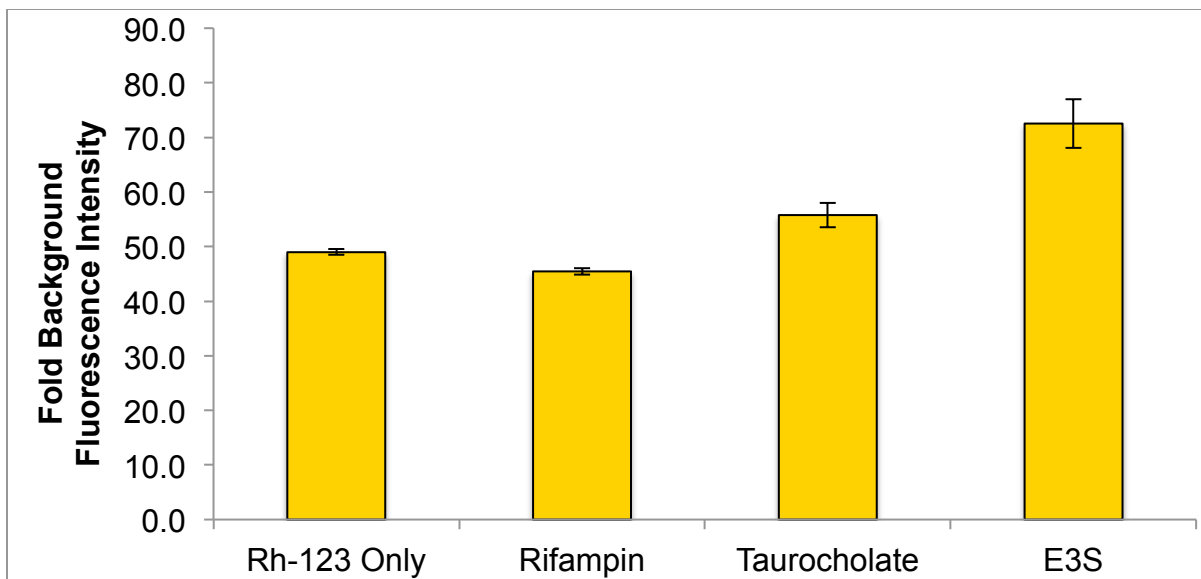


**Figure 13. Effects of OATP inhibitors on early rhodamine-123 uptake by PC3 cells.** Rhodamine-123 uptake by PC3 cells was not significantly inhibited by rifampin (0.1 mM), sodium taurocholate (0.3 mM), or estrone-3-sulfate (E3S, 0.3 mM) when incubated for 5 minutes at 37°C. Conversely, both taurocholate and E3S were shown to increase the amount of intracellular Rh-123. Data are the mean fold background fluorescence intensities and standard deviations of three biological replicates for each treatment. Each biological replicate value was the mean of three technical replicates ( $n = 1$ ).

To determine if Rh-123 uptake was truly indicative of OATP activity, an inhibition assay was performed on LNCaP cells grown in androgen-depleted conditions with an additional OATP1A2 inhibitor, ketoconazole. Only the ketoconazole (0.3 mM) treatment was shown to significantly inhibit Rh-123 uptake by these cells as the fold background fluorescence intensity of the corresponding lysate was 50.3% less than that of the Rh-123 only treatment (Figure 14). This result potentially validated the optimized fluorescence transport assay protocol used in this study as it was consistent with the findings of Arakawa et al.<sup>14</sup>

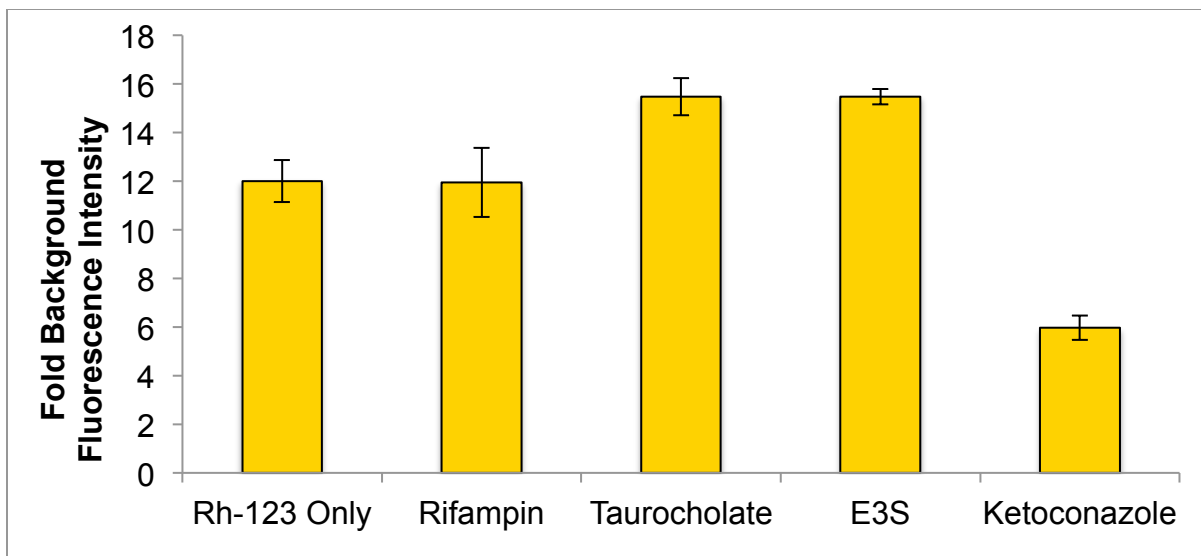


**Figure 14. Effects of OATP inhibitors on early rhodamine-123 uptake by LNCaP cells grown in androgen-depleted conditions.** Only ketoconazole was shown to significantly inhibit Rh-123 uptake by LNCaP cells grown in androgen-depleted conditions as the fold background fluorescence intensity of the cell lysate was 50.3% less than that of the Rh-123 only treatment. Data are the mean fold background fluorescence intensities and standard deviations of three biological replicates for each treatment. Each biological replicate value was the mean of three technical replicates ( $n = 1$ ).

## VII. Discussion

Understanding the biological mechanisms responsible for tumor metastasis and drug resistance is crucial for designing effective cancer therapies. The work in the present study was conducted to establish a project aimed at elucidating the potential roles of OATPs in invadopodia-associated tumor metastasis. The first step in exploring this query was to determine if OATPs are functionally expressed in a variety of invasive cancer cell lines. Before any of the aforementioned experiments were carried out, extracted membrane fractions from LNCaP, LNCaP overexpressing Tks5 (LNPT), PC3, Src-3T3, and SCC61 (head and neck cancer) cells were probed for OAT1 and OATP1B1 via Western Blot. At that time, neither of these transporters was detected. In addition, the transporters could not be identified in any of these cell lines via immunostaining with the same antibodies. These negative results could have stemmed from using un-optimized cell lysis, membrane extraction, and immunostaining protocols, which would explain why the positive control, caveolin, was also not detected. Alternatively, the protein levels of these transporters in cultured cells may simply be below the detection limit of the aforementioned antibody-based techniques. Instead of spending time optimizing these methods, a series of functional assays were employed.

Using fluorescence transport assays, Src-3T3, PC3, LNCaP, and MDA-MB-231 cell lines were shown to take up Rh-123 dye more effectively than any other dye tested. As Rh-123 is a substrate of OATP1A2, these results provided preliminary evidence of functional transporter expression.<sup>23</sup> In addition, the uptake of Rh-123 by the MDA-MB-231 and PC3 cell lines was likely to be mediated by a transporter(s)

since significantly less dye entered the cells when the experiment was carried out on ice compared to that at physiological temperature. This was interesting since previous reports indicated that MDA-MB-231 cells express low levels of OATP1A2 mRNA.<sup>28</sup> Furthermore, OATP1A2 expression was found to be heightened in less-invasive breast cancer cell lines. This, in conjunction with the fact that initial inhibition assays revealed that Rh-123 uptake by PC3 cells was not reduced in the presence of presumably saturating quantities of typical OATP1A2, 1B1, and 1B3 inhibitors, indicated that the uptake may be mediated by other unknown transporter(s).

The results of the preliminary inhibition experiments called into question the validity of the optimized fluorescence transport assay. In order to assess this possibility, another OATP1A2 inhibitor, ketoconazole, was acquired and used in a single fluorescence transport assay with LNCaP cells grown in androgen-depleted conditions.<sup>29</sup> Since Arakawa et al. indicated that OATP1A2 was upregulated in these conditions, it was hypothesized that OATP1A2-mediated transport would be easier to identify in this model system.<sup>14</sup> Here, Rh-123 uptake was significantly reduced by concentrated ketoconazole as the fluorescence signal of the corresponding lysate was 50.3% less than that of the dye-only treatment. While Arakawa et al. did not use ketoconazole, the results of our experiment also suggested enhanced OATP1A2 expression in these cells.<sup>14</sup> However, these researchers observed Rh-123 uptake was significantly inhibited by estrone-3-sulfate and taurocholate while these substances were shown to increase intracellular Rh-123 accumulation in the current work.

These conflicting results may arise from the inherent issues associated with fluorescence transport assays. First, since OATPs transport a wide variety of substances, it is possible that multiple transporters could be responsible for the observed Rh-123 uptake. Thus, while Rh-123 uptake is thought to be primarily mediated by OATP1A2 in HEK293 MSRII cells, not all of its potential transporters have been identified.<sup>23</sup> Another potential source of discrepancy arises from specific substrate-transporter interactions. Instead of Rh-123, Arakawa et al. used tritium-labeled DHEAS, which presumably has a different affinity for and clearance rate through OATP1A2 than Rh-123.<sup>14</sup> This is compounded by the fact that inhibitors frequently have different affinities for a given transporter. For example, for OATP1A2, estrone-3-sulfate reportedly has a  $K_m$  of 16  $\mu\text{M}$ , while that of Rh-123 is 0.3  $\mu\text{M}$ .<sup>23,30</sup> The varying affinities and  $V_{max}$  values of each substrate/transporter combination could be responsible for differential uptake efficiencies. While the kinetic data are not available for many OATP/inhibitor combinations, the possible effects of differential uptake efficiencies on apparent Rh-123 inhibition must be considered when establishing causality. It is also important to note that radiolabeled substrates are generally more ideal for transport assays than fluorescent ones because radiolabeled substrates yield less background signal and higher detection sensitivity comparatively.

More problems arise when one considers the fact that certain transporters like p-glycoprotein (p-gp) both export Rh-123 and are affected by OATP inhibitors.<sup>23</sup> For example, if p-glycoprotein were competitively inhibited by estrone-3-sulfate, Rh-123 export would be impeded, which would result in an inflated intracellular

concentration. Additionally, certain compounds like rifampin can induce p-gp activity, at least in the human intestine.<sup>31</sup> These problems associated with transporter-substrate kinetics could be partially ameliorated by overexpressing OATPs in the cells prior to the transport assay, a very common practice. This would accentuate the activity of the importer of interest and the results would be less affected by endogenous exporter activities. However, given the fact that ketoconazole is known to both inhibit OATP1A2 and p-gp, and a 50.3% reduction in fold background fluorescence intensity was observed in the present study, it was likely that ketoconazole inhibited Rh-123 import more than its export even at endogenous expression levels.<sup>29,32</sup> Interestingly, ketoconazole is also known to inhibit androgen biosynthesis and is used to treat castration-resistant prostate cancer which lends support to the putative relationship between OATP1A2-mediated androgen precursor transport and androgen resistance.<sup>33</sup> Thus, the combination of ketoconazole and Rh-123 transport assays may prove to be useful for assessing endogenous OATP1A2 activity in prostate cancer cells.

While Rh-123 has been used to study p-gp-mediated export, its use as an import protein tracer has not been extensively characterized. Historically, Rh-123 was believed to be membrane-permeable and thus able to enter the cell without the need for a protein carrier.<sup>23</sup> However, it was determined that passive diffusion is minimal and OATP1A2 activity predominates at concentrations below the micelle critical limit (2 µM). To reduce the possibility for passive diffusion, the final concentration of Rh-123 was chosen to be 0.3 µM in the current work. The time-course assay, in conjunction with a variety of drug and temperature inhibition

experiments, helped validate that the uptake of Rh-123 by PC3, MDA-MB-231, and LNCaP cells was indeed protein-mediated. It should also be noted that a previous report indicated that Rh-123 uptake by carcinoma cells was generally greater than that by the corresponding normal tissue, which potentially supports the idea that certain OATPs (specifically OATP1A2) are upregulated in cancer cell lines.<sup>34</sup>

Taken together, the previous results indicated that OATPs may have been present in the three cancer cell lines tested in this study. Since Arakawa et al.'s results indicated a potential connection between the OATP substrate DHEAS and AR activation, an experiment was conducted to determine the effects of AR stimulation on invadopodia morphology in Src-3T3 cells.<sup>14</sup> However, due to the fact that Src-3T3 cells exhibit highly developed, robust invadopodia, the effects of androgen receptor stimulation by R1881 were difficult to determine and therefore inconclusive. This could also potentially support the results of Zarif et al. that activated AR stimulates Src activity.<sup>20</sup> In this cell line, which expresses constitutively active Src, further Src activation by AR may have less of an effect on invadopodia regulation than it would in a cell line with unaltered Src levels. A more ideal model system for this experiment might be LNCaP cells overexpressing Tks5 (LNPT), an invadopodia promoter, however, at the time of this experiment, there was a problem with our stock LNPT viability. LNPT cells have less pronounced invadopodia and presumably lower activated Src levels and therefore invadopodia enhancement would be more readily apparent. If OATPs are found to contribute to invadopodia formation via a Src-AR pathway, they may serve as viable therapeutic targets.

## VIII. Future Work

In the future, inhibition assays will be performed on a variety of cell lines using various concentrations of ketoconazole to determine if the observed inhibition of Rh-123 uptake by LNCaP cells is a dose-dependent phenomenon. Assuming the effects of ketoconazole are dose-dependent, more OATP1A2 inhibitors can be purchased and employed to confirm that this transporter is responsible for the majority of the observed protein-mediated uptake of Rh-123. Once the OATPs (or similar classes of transporters) responsible for Rh-123 uptake have been identified, the effects of their inhibition and overexpression on invadopodia activity will be determined using gelatin degradation assays in conjunction with inhibitors and/or siRNA. An overview of this process is described in Figure 15.<sup>35</sup>

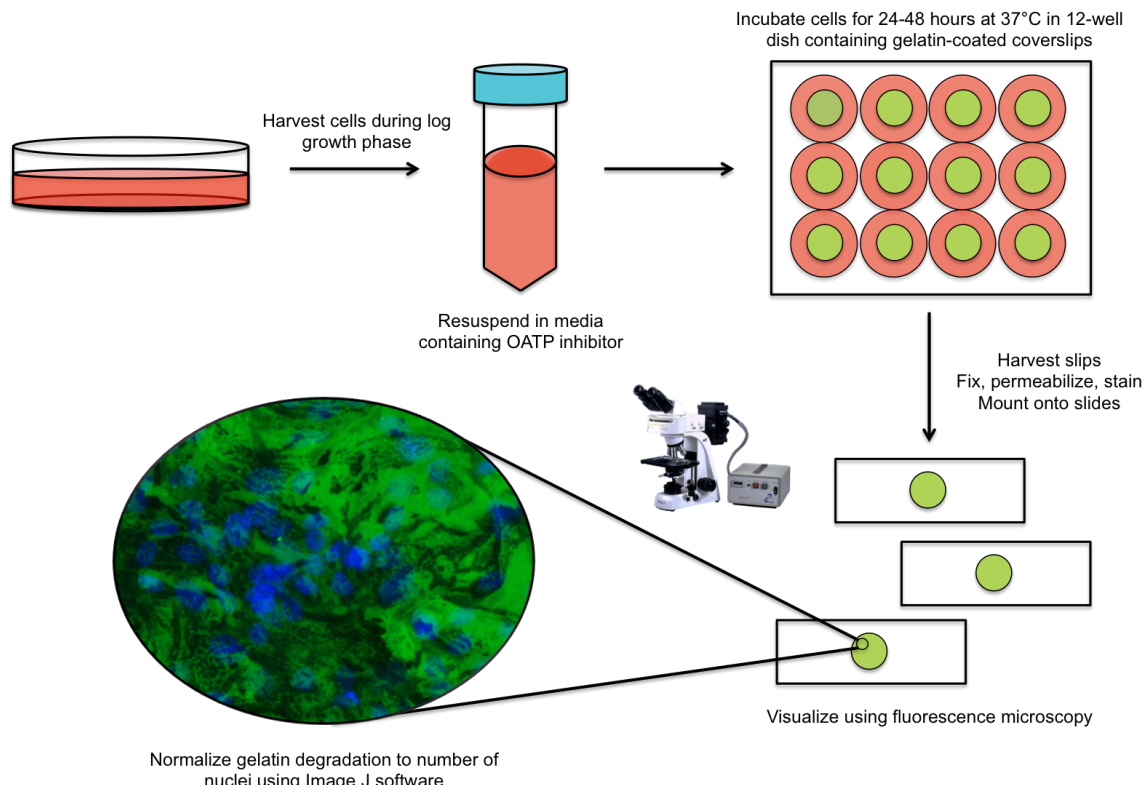


**Figure 15. Overview of the gelatin degradation assay protocol.**

The localization of OATPs during invadopodia formation may be determined by coexpressing these proteins with Src and Tks5, known invadopodia promoters, in a variety of cell lines. Immunofluorescence microscopy and immunoblotting will be employed to determine the cellular localization and expression of OATPs in invadopodia-competent cells respectively. Finally, the roles of OATPs in the development of the *C. elegans* vulva, an interesting *in vivo* invadopodia model, can be explored in future experiments.<sup>36</sup>

## **IX. Conclusion**

It is possible that OATPs (or similar drug transporters) are present in the invadopodia-competent cancer cells used in the present study since the uptake of Rh-123 by MDA-MB-231, PC3, and LNCaP cells was found to be protein-mediated using a series of temperature and drug uptake inhibition assays. Furthermore, the fact that Rh-123 uptake by LNCaP cells grown in androgen-depleted conditions was likely mediated by OATP1A2 potentially validated the fluorescence transport assay protocol optimized for mammalian cell lines that was used in this study. Previous reports have indicated that OATs (and assumedly OATPs) may be localized to invadopodia as both structures are associated with lipid rafts and caveolin-1. In the future, a series of inhibition assays will be performed to determine if OATPs contribute to invadopodia activity. In addition, the localization and expression of OATPs will be determined using fluorescence microscopy and Western blotting respectively. If OATPs are found to localize to invadopodia and contribute to both the drug-resistant and invasive phenotypes of aggressive cancer cells, they may be effective targets for therapy in the future.

## X. Acknowledgements

Special thanks to the ASU Office of Student Research for providing multiple Undergraduate Research Assistantships, research awards, and travel grants.

Thanks to the ASU Honors College for providing a Partnership Board Research grant that was used to purchase most of the dyes and inhibitors used in the present study. I was unbelievably fortunate to have learned from many outstanding mentors during my time at Appalachian State University. Thanks to Dr. Cartaya for convincing me to become a chemistry major when I was transitioning from pursuing music to science. Likewise, thanks to Dr. Douglas James, my guitar professor, for supporting me during this challenging time. Thanks to Dr. Babyak, both one of my readers and favorite chemistry teachers, who helped me develop my scientific writing abilities in her Quantitative Analysis lab. Thanks to Celeste Crowe and Dr. Leslie Jones for helping me to identify my passion while encouraging me along my path to medical school. Most students are lucky to form a close bond with one excellent research advisor. Somehow I was lucky to do so with two. I have learned many important skills from Drs. Jennifer Cecile and Darren Seals over the years and cannot express how grateful I am for having the opportunity to work with them.

Finally, thanks to my mom, Martha Brophy, and my brother, Trent Tabor, who have helped me through the rough spots. Everything I do is in memory of my father, George Roley Tabor, and I constantly work to make him proud.

## **XI. Biographical Sketch**

Travis was born on July 2, 1993 in Wilmington, NC to George and Martha Tabor. Upon graduating from John T. Hoggard High School in 2011, he attended Appalachian State University where he intended to pursue both classical guitar performance and physics degrees. After two years of intense study, he had to give up his dreams of being a guitarist due to overuse-related hand problems. While initially vexing, this challenge proved to change Travis' life for the better. After switching gears and changing majors to chemistry, he found a new, deeper passion for the medical sciences. Now, with the goal of pursing an MD/PhD in neural stem cell biology, he hopes to develop treatments for patients with debilitating memory disorders like that from which his father suffered. Travis will receive a B.S. in Chemistry and graduate summa cum laude with both departmental and university honors. After graduation, he will start work as a postbaccalaureate IRTA fellow at the National Institute of Childhood Health and Human Development in Bethesda, MD. Here he will study memory processing and synaptic plasticity in the lab of Dr. Dax Hoffman while enjoying the DC area and applying to MD/PhD programs.

## XII. References

1. Seals, D. F. *et al.* The adaptor protein Tks5/Fish is required for podosome formation and function, and for the protease-driven invasion of cancer cells. *Cancer Cell* **7**, 155–165 (2005).
2. Mehlen, P. & Puisieux, A. Metastasis: a question of life or death. *Nat. Rev. Cancer* **6**, 449–458 (2006).
3. Frittoli, E., Palamidessi, A., Disanza, A. & Scita, G. Secretory and endo/exocytic trafficking in invadopodia formation: the MT1-MMP paradigm. *Eur. J. Cell Biol.* **90**, 108–114 (2011).
4. Quest, A. F. G., Leyton, L. & Párraga, M. Caveolins, caveolae, and lipid rafts in cellular transport, signaling, and disease. *Biochem. Cell Biol. Biochim. Biol. Cell.* **82**, 129–144 (2004).
5. Yamaguchi, H. *et al.* Lipid rafts and caveolin-1 are required for invadopodia formation and extracellular matrix degradation by human breast cancer cells. *Cancer Res.* **69**, 8594–8602 (2009).
6. Simons, K. & Ikonen, E. Functional rafts in cell membranes. *Nature* **387**, 569–572 (1997).
7. Simons, K. & Sampaio, J. L. Membrane organization and lipid rafts. *Cold Spring Harb. Perspect. Biol.* **3**, a004697 (2011).
8. Yamaguchi, H. & Oikawa, T. Membrane lipids in invadopodia and podosomes: key structures for cancer invasion and metastasis. *Oncotarget* **1**, 320–328 (2010).

9. Caldieri, G. *et al.* Invadopodia biogenesis is regulated by caveolin-mediated modulation of membrane cholesterol levels. *J. Cell. Mol. Med.* **13**, 1728–1740 (2009).
10. Roth, M., Obaidat, A. & Hagenbuch, B. OATPs, OATs and OCTs: the organic anion and cation transporters of the SLCO and SLC22A gene superfamilies. *Br. J. Pharmacol.* **165**, 1260–1287 (2012).
11. Nakanishi, T. & Tamai, I. Putative roles of organic anion transporting polypeptides (OATPs) in cell survival and progression of human cancers. *Biopharm. Drug Dispos.* **35**, 463–484 (2014).
12. Srimaroeng, C., Cecile, J. P., Walden, R. & Pritchard, J. B. Regulation of renal organic anion transporter 3 (SLC22A8) expression and function by the integrity of lipid raft domains and their associated cytoskeleton. *Cell. Physiol. Biochem.* *Int. J. Exp. Cell. Physiol. Biochem. Pharmacol.* **31**, 565–578 (2013).
13. Köck, K. *et al.* Rapid modulation of the organic anion transporting polypeptide 2B1 (OATP2B1, SLCO2B1) function by protein kinase C-mediated internalization. *J. Biol. Chem.* **285**, 11336–11347 (2010).
14. Arakawa, H. *et al.* Enhanced expression of organic anion transporting polypeptides (OATPs) in androgen receptor-positive prostate cancer cells: possible role of OATP1A2 in adaptive cell growth under androgen-depleted conditions. *Biochem. Pharmacol.* **84**, 1070–1077 (2012).
15. Hotte, S. J. & Saad, F. Current management of castrate-resistant prostate cancer. *Curr. Oncol.* **17**, S72–S79 (2010).

16. Castoria, G. *et al.* Androgen-induced cell migration: role of androgen receptor/filamin A association. *PLoS One* **6**, e17218 (2011).
17. Abram, C. L. *et al.* The adaptor protein fish associates with members of the ADAMs family and localizes to podosomes of Src-transformed cells. *J. Biol. Chem.* **278**, 16844–16851 (2003).
18. Guo, Z. *et al.* Regulation of androgen receptor activity by tyrosine phosphorylation. *Cancer Cell* **10**, 309–319 (2006).
19. Asim, M., Siddiqui, I. A., Hafeez, B. B., Baniahmad, A. & Mukhtar, H. Src kinase potentiates androgen receptor transactivation function and invasion of androgen-independent prostate cancer C4-2 cells. *Oncogene* **27**, 3596–3604 (2008).
20. Zarif, J. C., Lamb, L. E., Schulz, V. S., Nollet, E. A. & Miranti, C. K. Androgen receptor non-nuclear regulation of prostate cancer cell invasion mediated by Src and matriptase. *Oncotarget* **6**, 6862–6876 (2015).
21. El Baraka, M., Deumié, M., Viallet, P. & Lampidis, T. J. Fluorescence properties and partitioning behaviour of esterified and unesterified rhodamines. *J. Photochem. Photobiol. Chem.* **62**, 195–216 (1991).
22. Wang, J. *et al.* Development of high-throughput cell-based assays to study regulatory authority recommended SLC transporters. (2013).
23. Forster, S., Thumser, A. E., Hood, S. R. & Plant, N. Characterization of rhodamine-123 as a tracer dye for use in in vitro drug transport assays. *PLoS One* **7**, e33253 (2012).

24. Chow, A., Kennedy, J., Pottier, R. & Truscott, T. Rhodamine 123 – photophysical and photochemical properties. *Photobiochem. Photobiophys.* **11**, 139–148 (1986).
25. Choi, M.-K. *et al.* Inhibitory effects of ketoconazole and rifampin on OAT1 and OATP1B1 transport activities: considerations on drug-drug interactions. *Biopharm. Drug Dispos.* **32**, 175–184 (2011).
26. Schneider, C. A., Rasband, W. S. & Eliceiri, K. W. NIH Image to ImageJ: 25 years of image analysis. *Nat. Methods* **9**, 671–675 (2012).
27. Fluo-3, AM, Calcium Indicator - Thermo Fisher Scientific. Available at: <https://www.thermofisher.com/order/catalog/product/F1242>. (Accessed: 30th April 2016)
28. Wlcek, K. *et al.* Altered expression of organic anion transporter polypeptide (OATP) genes in human breast carcinoma. *Cancer Biol. Ther.* **7**, 1450–1455 (2008).
29. Taub, M. E. *et al.* Digoxin is not a substrate for organic anion-transporting polypeptide transporters OATP1A2, OATP1B1, OATP1B3, and OATP2B1 but is a substrate for a sodium-dependent transporter expressed in HEK293 cells. *Drug Metab. Dispos. Biol. Fate Chem.* **39**, 2093–2102 (2011).
30. Lee, W. *et al.* Polymorphisms in human organic anion-transporting polypeptide 1A2 (OATP1A2): implications for altered drug disposition and central nervous system drug entry. *J. Biol. Chem.* **280**, 9610–9617 (2005).

31. Westphal, K. *et al.* Induction of P-glycoprotein by rifampin increases intestinal secretion of talinolol in human beings: a new type of drug/drug interaction. *Clin. Pharmacol. Ther.* **68**, 345–355 (2000).
32. Zhang, Y., Hsieh, Y., Izumi, T., Lin, E. T. & Benet, L. Z. Effects of ketoconazole on the intestinal metabolism, transport and oral bioavailability of K02, a novel vinylsulfone peptidomimetic cysteine protease inhibitor and a P450 3A, P-glycoprotein dual substrate, in male Sprague-Dawley rats. *J. Pharmacol. Exp. Ther.* **287**, 246–252 (1998).
33. Keizman, D., Huang, P., Carducci, M. A. & Eisenberger, M. A. Contemporary experience with ketoconazole in patients with metastatic castration-resistant prostate cancer: clinical factors associated with PSA response and disease progression. *The Prostate* **72**, 461–467 (2012).
34. Nadakavukaren, K. K., Nadakavukaren, J. J. & Chen, L. B. Increased rhodamine 123 uptake by carcinoma cells. *Cancer Res.* **45**, 6093–6099 (1985).
35. Vozza-Brown, L., Grepper, S. & Sahi, J. Suppression of OATP1B1, OATP1B3, and OATP2B1 transporters in primary cryopreserved human hepatocytes following lipid delivery of stealth siRNA. (2009).
36. Morrissey, M. A., Hagedorn, E. J. & Sherwood, D. R. Cell invasion through basement membrane: The netrin receptor DCC guides the way. *Worm* **2**, e26169 (2013).